SURFACE WAVE IDENTIFICATION RESEARCH IN THE MIDDLE EAST AND NORTH AFRICA

Michael E. Pasyanos, Peter Goldstein, William R. Walter and Arthur Rodgers
Lawrence Livermore National Laboratory

Sponsored by U.S. Department of Energy
Office of Nonproliferation and National Security
Office of Research and Development
Nuclear National Security Administration

Contract No. W-7405-ENG-48

ABSTRACT

We are in the process of making improvements in surface wave identification throughout the Middle East and North Africa. Seismic surface waves have long played an important role in nuclear explosion monitoring by providing both information about the lithosphere they pass through and the source that generated them. We have made high-resolution group velocity maps of the Middle East and North Africa using the tomographic inversion of more than 10,000 individual path measurements. These maps provide valuable constraints on models of the underlying structure of the region. The maps also provide estimates of expected phase of new events that can be used in phase-match filters to compress the expected signal and thus improve the signal-to-noise ratio. Of very high interest is improving the performance of the traditional M_S:m_b discriminant and extending the discriminant down to events with smaller magnitude that are recorded at closer regional distances. This paper directly addresses the improvement that phase match filters bring to the estimation of the surface wave magnitude, M_S. We have estimated M_S for over 8000 events at 30 stations, both with and without the use of phase match filters, and have found a marked improvement in our ability to discriminate between earthquakes and explosions.

When considering smaller magnitude events, however, several other problems emerge. In our analysis, for example, deep events can flag as "explosion-like" using the m_b:M_S discriminant, since they are also inefficient generators of surface waves. If unidentified as deep events or classified as "normal" depth events, they can contaminate the actual distribution of surface wave magnitudes (and their derived discriminants) for shallow earthquakes. It is clearly very important to independently identify the source depth of these events in order to avoid misclassifying them. One possible method is through the use of waveform modeling. In order to be effective, however, we need to have reasonable estimates of local earth structure. We are also making use of a combined regional and teleseismic technique to provide constraints on source and structure. Far regional and teleseismic data provide high-resolution estimates of depth, while regional data help constrain the mechanism and structure.

Research performed under the auspices of the U.S. Department of Energy at the Lawrence Livermore National Laboratory under contract number W-7405-ENG-48.

Key Words: identification, surface waves, group velocity, discrimination, Middle East, North Africa

OBJECTIVE

The purpose of this study is to use surface waves to improve the identification of events throughout the Middle East and North Africa (MENA). We have calculated surface wave magnitude (Ms) from data in the LLNL MENA waveform database by measuring the amplitude of the surface wave train in specific period ranges. Amplitudes are then converted to magnitudes by a scale that accounts for factors such as period, attenuation, geometrical spreading, etc. Regional determinations of this parameter have proved difficult due to factors such as unsuitable magnitude algorithms, poor signal-to-noise, and propagation complications. We have tried to overcome some of these obstacles by using phase-matched filtering on the raw waveform and a surface wave magnitude algorithm suitable for regional distances.

Surface wave magnitude is an accurate measure of the long-period and shear-wave energy of a seismic event. It is generally used in conjunction with other magnitude estimates to form a discriminant. M_S:m_b is a well-known, important, and reliable discriminant between earthquakes and explosions. By calculating regional surface wave magnitudes, we hope to extend the threshold of the M_S:m_b discriminant down to lower magnitude levels. Discrimination between earthquakes and explosions is important to monitoring the Comprehensive Nuclear-Test-Ban Treaty.

RESEARCH ACCOMPLISHED

Surface wave magnitudes

We have selected all available waveform data for shallow (depth < = 50 km) events greater than or equal to m_b 3.5 from the LLNL MENA waveform database recorded at selected stations. A map of the stations and events used is shown in Figure 1. Stations are indicated by triangles. Events with only one or two single station measurements are shown in open circles. Events recorded with acceptable signal-to-noise ratio at three or more stations are shown in closed circles. Explosions, regardless of the number of recording stations, are indicated by the closed diamonds. Amplitude measurements are made by taking vertical waveforms containing surface waves and deconvolving them to ground displacement. The displacement traces are then bandpass filtered over a selected period range, usually around 20 seconds. The maximum amplitude and period of the surface wave is then measured.

In addition to making amplitude measurements on raw traces, we also measured amplitudes on traces that had been phase-matched filtered. The filtering routine compresses the signal using the input group velocity profile, eliminates any spurious energy occurring outside of the allowable frequency-time windows, and redisperses the cleaned signal. Phase-matched filter estimates are determined from surface wave group velocity estimates (Pasyanos et al., 2000). In previous studies (Pasyanos et al., 1999), we have also compared the results made using the high-resolution tomography in the Middle East to other estimates from a global surface wave model (Stevens and McLaughlin, 1997) and a 1-D global earth model PREM (Dziewonski and Anderson, 1981). Amplitude measurements are corrected for factors such as attenuation, geometrical spreading, and the period of the measurement in order to yield magnitude. Traditionally, M_S measurements (i.e. Gutenberg, IASPEI) are only made at teleseismic distances ($\Delta >$ 20°). Several methods have been developed to make regional surface wave measurements. We employ the formula of Rezapour and Pearce (1998), given as:

$$M_S = \log(A/T)_{max} + 1/3 \log(\Delta) + 1/2 \log(\sin \Delta) + 0.0046\, \Delta + 5.370$$

where A is amplitude, T is period, and Δ is distance in degrees.

Single station measurements for a given event are then combined in order to produce an overall magnitude for the event. We test three combination methods. The first is a network average, determined by calculating the mean of the individual measurements. Uncertainty is given as the standard deviation of the measurements. The second method that we test uses a maximum likelihood method to compensate for the self-censoring of data that occurs near the noise floor. Here we use the signal-to-noise ratio as a weighting function for the magnitude measurements. The third method that we used simply uses the maximum of the individual measurements as the event magnitude. The uncertainty used is the difference between the maximum measurement and the mean. While the second methodology will consistently overestimate magnitudes relative to the first method, this value might produce a better discriminant, the reasoning being that an observation of a large surface wave should not be down-weighted by other observations with small or non-existent surface waves. We have excluded any single station measurements derived from amplitudes with signal-to-noise ratios less than 0.65. While it may seem counterproductive to include any measurements with a signal-to-noise ratio of less than 1.0 (or higher), we choose to keep events near the threshold since it is the absence of surface wave signal which is the discriminant. Although events with very low signal-to-noise ratios (< 0.65) will have such small weights in the maximum likelihood method as not to significantly influence the event magnitude, they have been completely removed so as not to contaminate single station measurements or magnitude estimates made using the other (mean and maximum) methods, where the effect would be severe.

Overall, we have made over 49,000 amplitude estimates for over 8,000 events at 30 stations using 4 different methods (without phase-matched filtering and with phase-matched filtering using three different models). Consequently, we have made over 8,000 single-station magnitude estimates with acceptable signal-to-noise ratio. This results in a total of 7,000 earthquakes with 2 or more stations and about 6,000 earthquakes with 3 or more stations, along with 8 explosions. In conjunction with other high-frequency magnitude estimates (i.e. m_b), M_S forms an important discriminant between earthquakes and explosions. In order to test and validate our results, we have taken the measured surface wave magnitudes for a particular station and compared them against m_b measurements taken from the USGS PDE catalog. Figure 2 shows plots of M_S:m_b for events which have been phase-matched filtered using the group velocities predicted from the surface wave tomography. Event magnitudes have been calculated using the maximum likelihood method. Explosions are indicated by the blue diamonds. For a given m_b, explosions produce M_S measurements that are low. The best fitting regression of the measurements is shown by the solid line. We calculate our discriminant by subtracting from the measured surface wave magnitude the surface wave magnitude expected from the body wave magnitude, as determined from the regression line in Figure 2. Explosions generally have M_S measurements between one and two magnitude units lower than earthquakes with a similar body wave magnitude.

We perform a simple statistical analysis on both the earthquakes and explosions to estimate the mean and variance of the discriminant in the two populations (Figure 3a). From the statistics of the two populations, we can now generate receiver operator curves. A receiver operator curve quantifies the probabilities of misidentifying events with a particular discriminant, either as an explosion misclassified as an earthquake (missed violation) or as an earthquake misclassified as an explosion (false alarm). The receiver operator curve is asymmetric due to the unequal variances in the earthquake and explosion populations. Figure 3b shows the corresponding receiver operator curve for the two statistical populations. The equiprobable point is defined as the point on the curve where the missed violation rate and the false alarm rate are equivalent. Without phase-matched filtering and maximum likelihood we have an equiprobable point of 0.116 or 11.6%. Using maximum likelihood, the equiprobable point increases slightly to 0.128 or 12.8%. When we use phase-matched filtering without maximum likelihood, the equiprobable point drops to 0.080 or 8.0%. Finally, using phase-matched filtering and maximum likelihood, we find an equiprobable point of 0.080 or 8.0%. This is the solid curve shown in Figure 3b. The dashed curve corresponds to the equiprobable line with no phase matched filtering. This quantifies the improvement in M_S-m_b discrimination provided by phase-matched filtering using the LLNL group velocity maps and correction surfaces. We expect that phase-matched filtering will become of premium importance for the smallest magnitude events.

Investigating anomalous events

Differences in surface wave and body wave magnitudes can be caused by a number of factors. Events with deep source depths do not effectively generate surface waves and will flag as anomalous events. Some events in this database from the Hindu Kush and Zagros regions that were tagged with nominal source depths (i.e. 10 km, 33 km) fall into this category (see Figure 4). Since their source depths can often be determined independently by other means, they can be ruled out as explosions by other means. If these deep events can be systematically identified and removed from the earthquake population, we would expect to see even greater separation between the two populations.

Figure 5 shows a plot of the M_S:m_b discriminant as a function of catalog source depth. Earthquakes are illustrated by the triangles and explosions by the stars. There are a couple of features to note. First, there is a clear trend in the discriminant with depth. This trend is unsurprising since we expect deeper events to be less efficient producers of surface waves than shallower events, and this is reflected here. The trend results in about a 1.0 unit difference in the discriminant between 0 and 50 km depth. Secondly, with the exception of the Pakistani explosion which occurred in the coda of a large nearby shallow earthquake in Afghanistan, the explosions separate well from the earthquake population, particularly with respect to other shallow events. Finally, we can see the large scatter from earthquakes where the depth was unknown, but arbitrarily set to a particular depth by a geophysicist. These are represented by the large bands occurring at 5 km, 10 km, and especially at 33 km. In these cases, most of the events that are indicated as explosion-like are probably deep events, especially in light of the fact that most of these events are happening in areas where deep events are known to occur. For example, if the trend that we are seeing in the discriminant continues to deeper events, then a mislocation in source depth from 130 km to 33 km could make a difference of about 2 units in the discriminant, bringing those events back into the middle of the population. Even a mislocation of about 50 km in depth would clearly put the event back into the scatter in the earthquake population.

Figure 6 is an example of an event in the Hindu Kush region that had a 33 km source depth and an anomalously low M_S. Waveform modeling was performed on data at station NIL, located about 150 km south of the event. We suspected that this event might be deep, causing the large discrepancy in magnitudes. Results from the waveform modeling indicate otherwise, suggesting a source depth of about 25 km. Another possible explanation for the anomaly is that the attenuation relationship used in the Rezapour and Pearce magnitude formula might not be appropriate for all areas. The thick crust in the Hindu Kush region differs significantly from the global average for the crust. This effect is particularly critical when we are considering events located close in to the seismic stations, as we are in this particular case. Several other possibilities exist. One is that the m_b for this event is significantly overestimated, producing a larger m_b-M_S discrepancy. For an m_b 5.0 event, this earthquake did not produce very large signals at regional recording stations. In addition to being close, several of the nearest stations also appear to be nodal for the Rayleigh wave, as station NIL is in Figure 6. This would also cause an underestimate of M_S. We would like to estimate the source depth of as many of these events with constrained depth as possible and, if necessary, to properly remove them from the earthquake population. There are still a number of unresolved questions of why many of the events in particular regions are anomalous. Sorting out these issues is an active research area.

CONCLUSIONS AND RECOMMENDATIONS

Using surface wave magnitudes in discriminants has long been important in identifying seismic events. By employing techniques such as phase-matched filtering that has been based on high-resolution tomographic studies, we can begin to also apply this capability to smaller, regional events. As our understanding of regional earth structure improves, we can expect to see continued improvement in regional discriminants using surface waves. As illustrated in our study, it is imperative to the success of this discriminant to be able to independently identify and remove deeper events that also flag as “explosion-like.” While large events often have clear indications of the source depth, such as depth phases, these signals are often obscured for smaller events. We are considering several methodologies to help us in this endeavor.

REFERENCES

Dziewonski, A. and D. Anderson, Preliminary Reference Earth Model, Phys. Earth. Planet. Int., 25, 297-356, 1981.

Pasyanos, M.E., W.R. Walter, S.R. Ford, S.E.Hazler, Improving mb:Ms Discrimination using Phase Matched Filters Derived from Regional Group Velocity Tomography, 21st Seismic Research Symposium, September 21-24, 1999, Las Vegas, NV.

Pasyanos, M.E., W.R. Walter, and S.E. Hazler, Surface wave dispersion study of the Middle East and North Africa for Monitoring the Comprehensive Nuclear-Test-Ban Treaty, LLNL Report UCRL-JC-133973, submitted to Pure and Applied Geophysics, 2000.

Rezapour, M. and R.G. Pearce, Bias in Surface-Wave Magnitude Ms due to Inadequate Distance Corrections, Bull. Seism. Soc. Am., 88, 43-61, 1998.

Stevens, J. and K. McLaughlin, Improved methods for regionalized surface wave analysis, Final Report PL-TR-97-2135, Phillips Laboratory, Directorate of Geophysics, AFMC, Hanscom AFB, 26 pp., 1997.

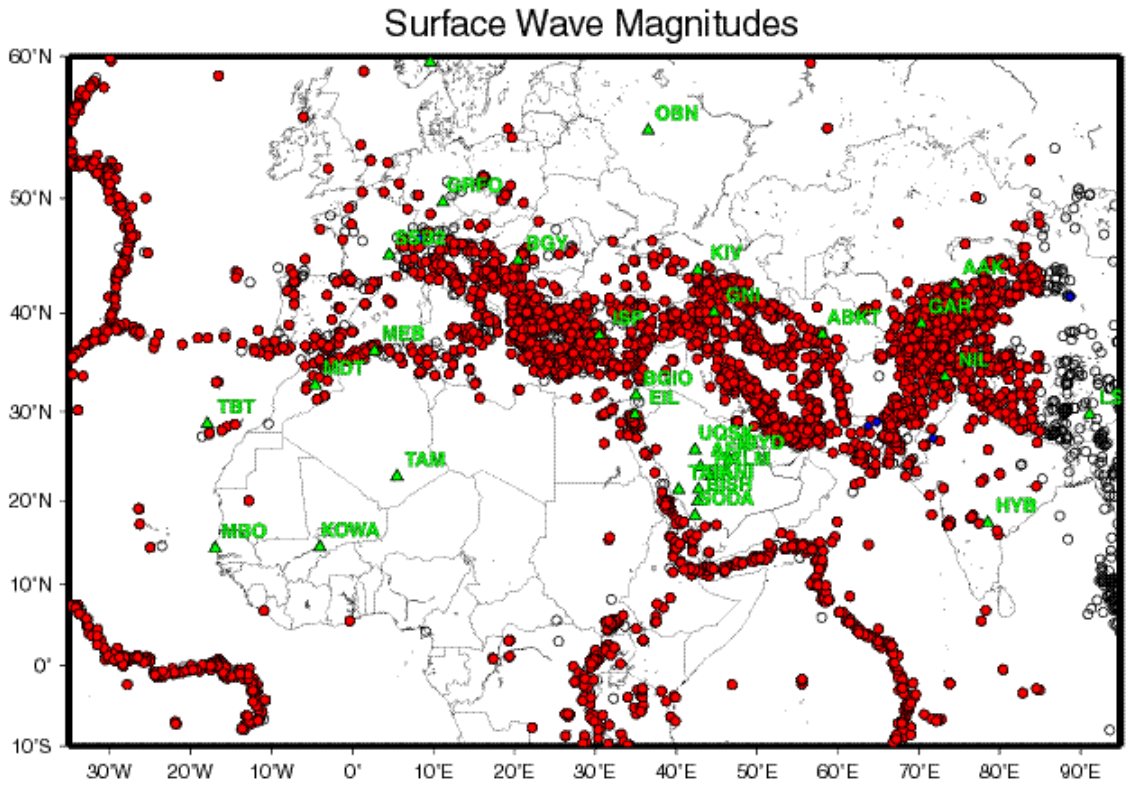

Figure 1. Events and stations used for surface wave magnitudes. Stations are indicated by triangles. Events are shown by circles, explosions are indicated by the solid diamonds.

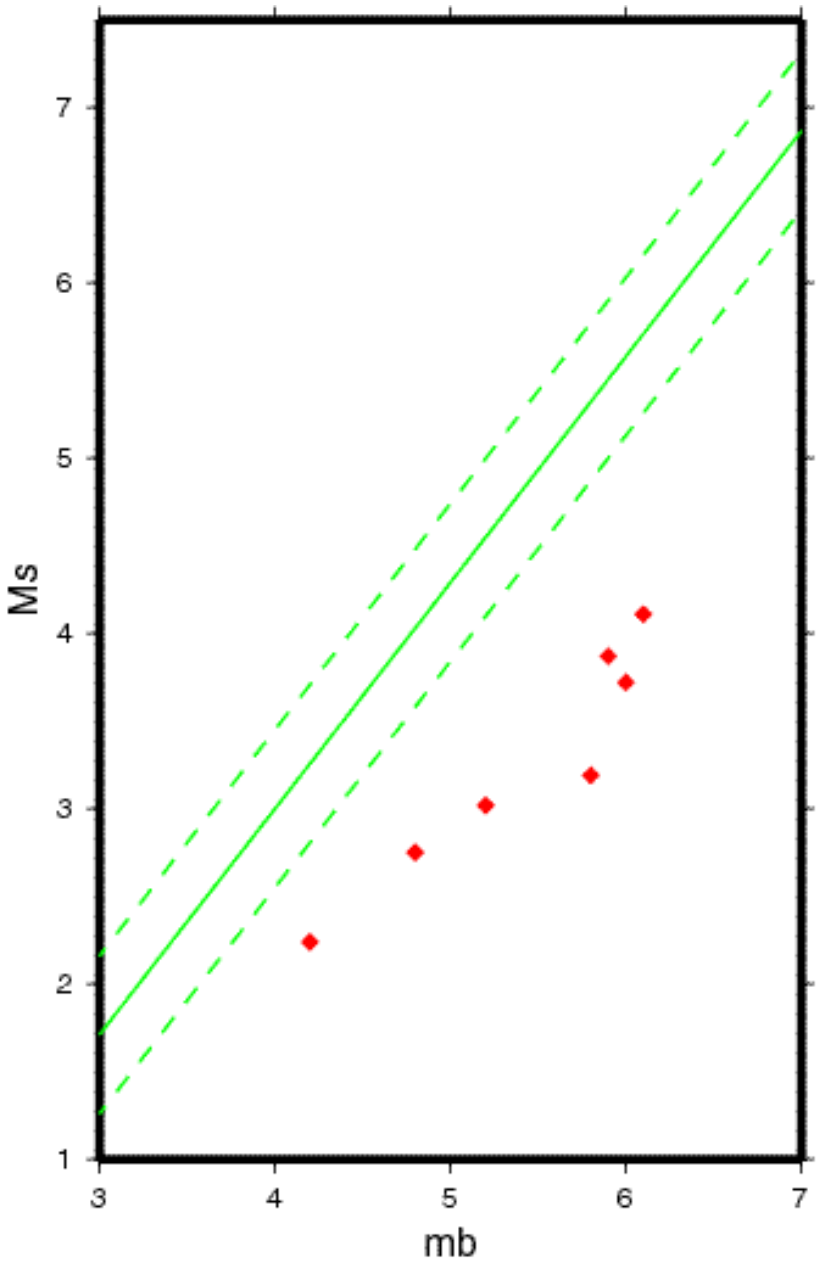

Figure 2. Plot of mb vs. Ms for events which have been phase-matched filtered using the group velocities predicted from the surface wave tomography. The best fitting regression of the earthquakes (not shown) and one standard deviation are shown by the solid and dashed green lines. Explosions are indicated by the red diamonds.

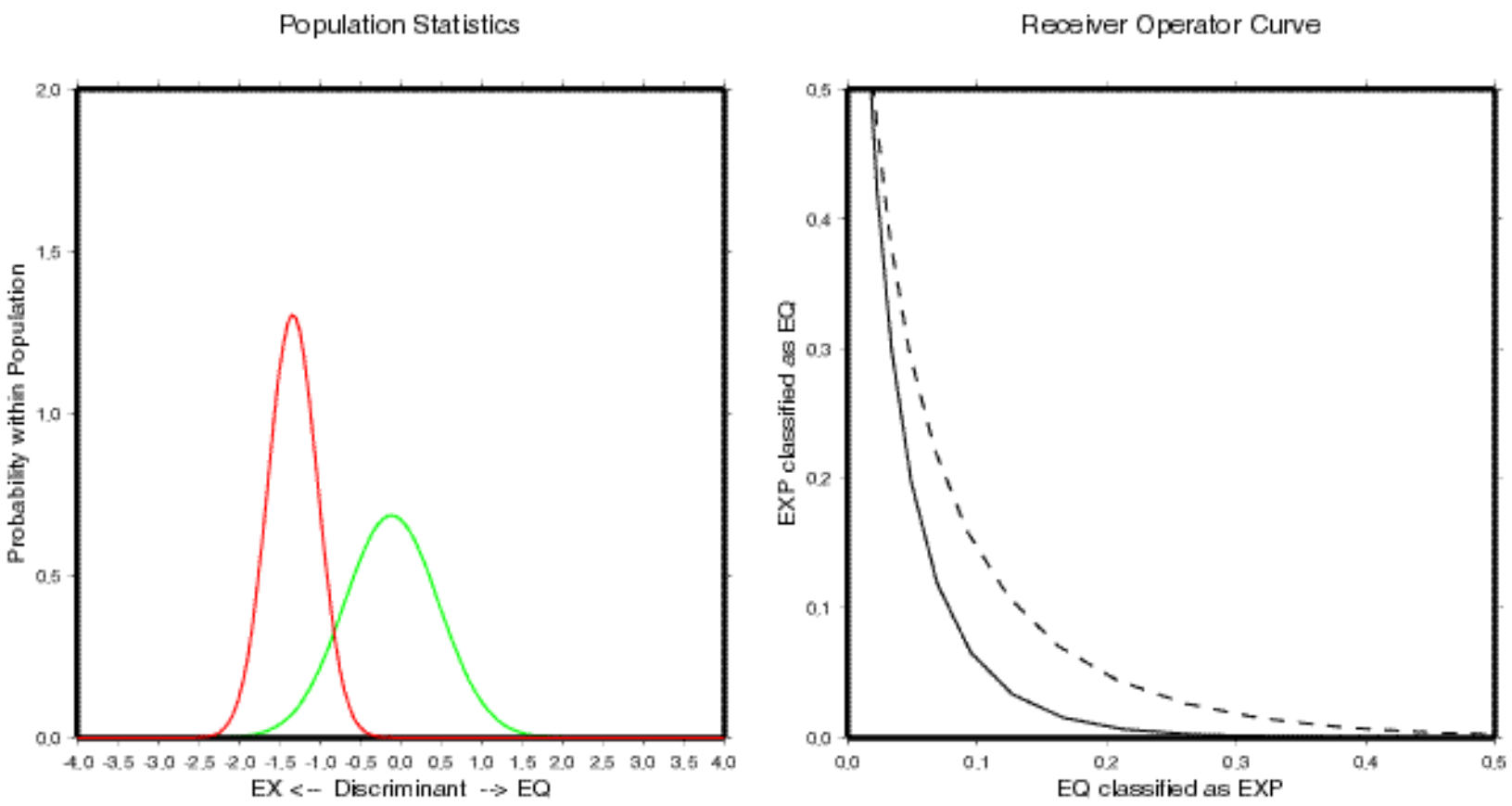

Figure 3. Separation of the discriminant for the earthquake (green curve) and explosion (red curve) populations and the receiver operator curves derived from the statistics of the discrimant for the two populations. The solid curve corresponds to the receiver operator curve with phase-matched filtering and the dashed line corresponds to the reciver operator curve with no phase-matched filtering.

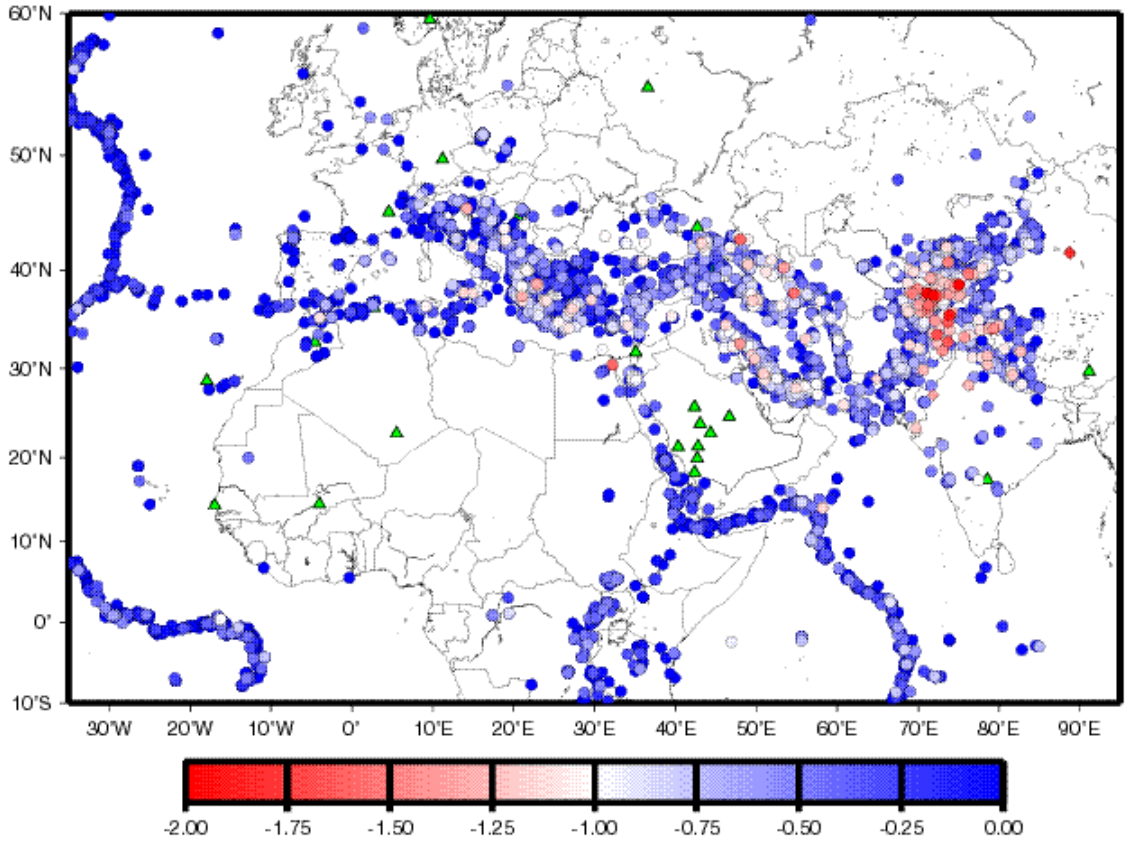

Figure 4. Map view of events color coded by Ms:mb discriminant. Earthquake-like events are shown in blue shades, explosion-like events are in red shades. Stations are shown as green triangles.

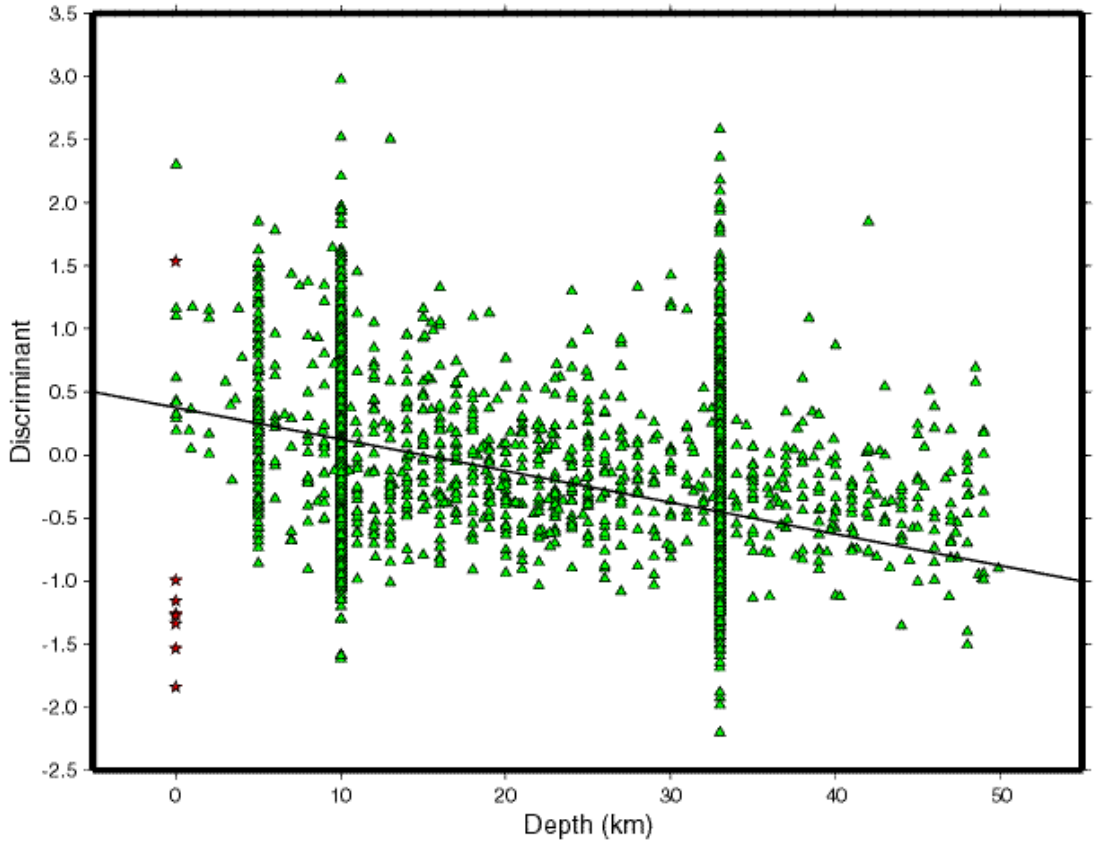

Figure 5. Discriminant plotted as a function of source depth. Earthquakes are illustrated by green triangles, explosions by the red stars. Large scattering in the discriminant are found where the depths are fixed at 5 km, 10 km, and especially at 33 km.

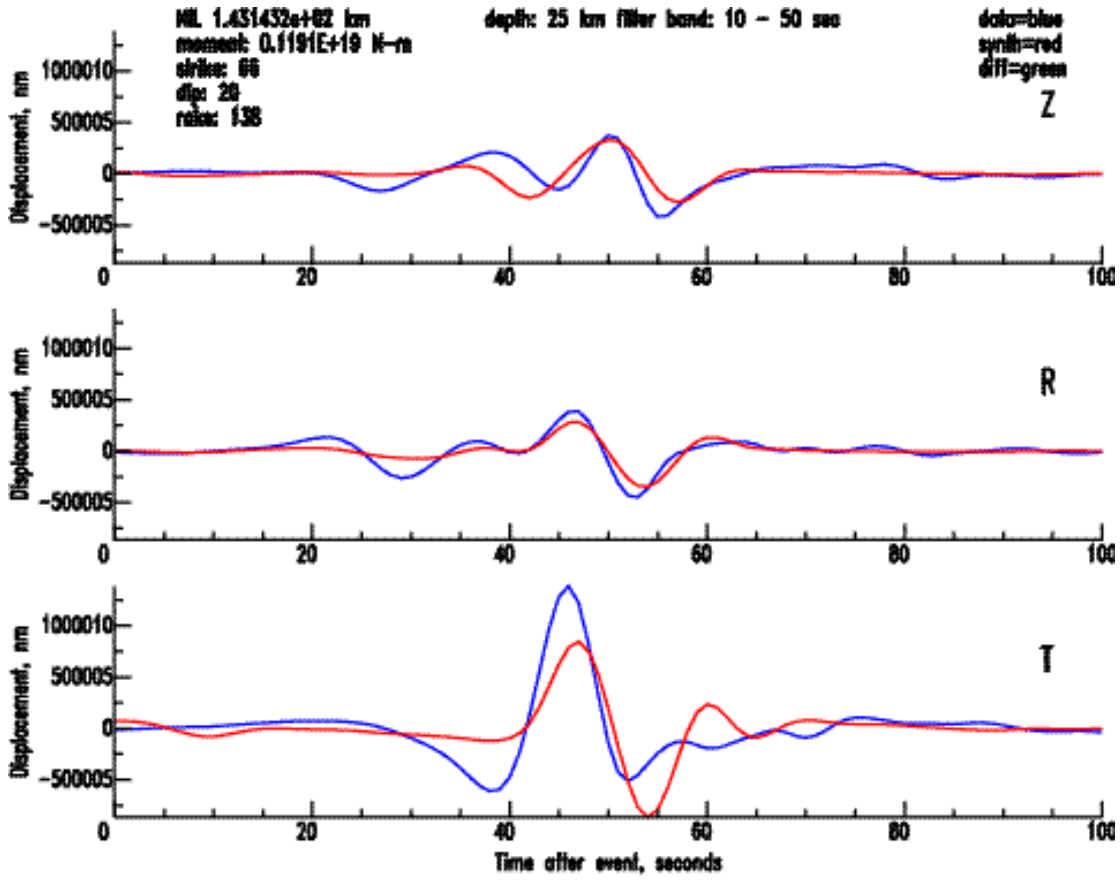

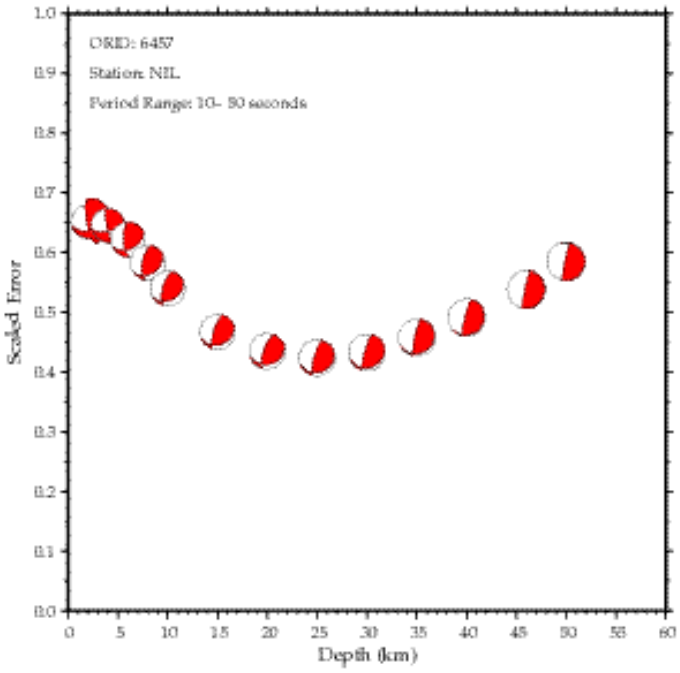

Figure 6. Waveform modeling results for an anomalous event in the Hindu Kush.